

# 1 **The emergence of supergenes from inversions in Atlantic salmon.**

2  
3 Kristina Stenlkk, Marie Saitou, Live Rud-Johansen, Torfinn Nome, Michel Moser, Mariann rnyasi, Matthew  
4 Kent, Nicola Jane Barson\* and Sigbjrn Lien\*.

5  
6 \*contributed equally as senior and corresponding author

7  
8 Centre for Integrative Genetics (CIGENE) and Department of Animal and Aquacultural Sciences,  
9 Faculty of Biosciences,  
10 Norwegian University of Life Sciences

## 11 12 13 **Abstract**

14 Supergenes link allelic combinations into non-recombining units known to play an essential role in  
15 maintaining adaptive genetic variation. However, because supergenes can be maintained over millions of  
16 years by balancing selection and typically exhibit strong recombination suppression, both the underlying  
17 functional variants and how the supergenes are formed are largely unknown. Particularly, questions remain  
18 over the importance of inversion breakpoint sequences and whether supergenes capture preexisting  
19 adaptive variation or accumulate this following recombination suppression. To investigate the process of  
20 supergene formation, we identified inversion polymorphisms in Atlantic salmon by assembling eleven  
21 genomes with nanopore long-read sequencing technology. A genome assembly from the sister species,  
22 brown trout, was used to determine the standard state of the inversions. We found evidence for adaptive  
23 variation through genotype-environment associations, but not for the accumulation of deleterious  
24 mutations. One young 3Mb inversion segregating in North American populations, has captured adaptive  
25 variation that is still segregating within the standard arrangement of the inversion, while some adaptive  
26 variation has accumulated after the inversion. This inversion and two others had breakpoints disrupting  
27 genes. Three multigene inversions with matched repeat structures at the breakpoints did not show any  
28 supergene signatures, suggesting that shared breakpoint repeats may obstruct supergene formation.

## 29 30 **Keywords**

31 Inversion, supergene, Atlantic salmon, long-read sequencing, adaptive variation, population differentiation

## 32 33 **Introduction**

34 Supergenes are clusters of linked alleles which segregate as if they were a single locus and that determine  
35 alternate phenotypes in balanced polymorphisms [1]. They can evolve in regions of suppressed  
36 recombination caused by structural variation, including inversions, insertions and deletions where the  
37 linkage among favourable combinations of alleles is increased [2]. Chromosomal inversions are increasingly  
38 recognized as important for adaptation across taxa [1, 3-8] and often underlie supergenes. However,  
39 suppressed recombination makes them particularly vulnerable to the accumulation of recessive deleterious  
40 mutations and these may be key to supergene persistence through increased heterozygote fitness [2, 4].  
41 Furthermore, breakpoints mutations themselves can have direct phenotypic effects [5, 7, 8] making it unclear  
42 which processes lead to the development of supergenes. The suppressed recombination that is central to  
43 supergene development hinders the dissection of the events leading to their formation. Many iconic  
44 supergenes are relatively old, (e.g. >1MY [3, 5]) obscuring the sequence of events leading to their  
45 development. Despite increasing numbers of supergenes being detected, the early stages of supergene  
46 formation remain poorly understood.

47  
48 Inversion supergenes can be maintained by various forms of balancing selection. For example, sexual  
49 antagonism [3, 9], negative frequency dependent selection [5, 8], temporally and spatially varying  
50 selection [3, 4] and heterozygote advantage [4]. These different forms of balancing selection can combine to  
51 promote supergene persistence [4] and their importance can change over the lifespan of the inversion [10].  
52 Spatial variation in selection with migration can lead to a form of balancing selection, migration-selection  
53 balance, which can maintain inversion polymorphisms [11]. This is an attractive model as it explains both the

54 initial invasion, and subsequent maintenance as a polymorphism using a widespread process. When an  
55 inversion first occurs, and is rare, it is vulnerable to being lost by genetic drift or selection if it causes  
56 deleterious effects. The capture of locally adapted variation has been shown to increase the probability of  
57 an inversion increasing in frequency, however there is little empirical evidence to support its occurrence [12]  
58 (but see [6, 13]). Recombination suppression in inversions complicates the identification of the variants  
59 underlying their effects and the age of many inversions make it difficult to determine whether adaptive  
60 variation was present before the inversion occurred or accumulated afterwards. Likewise, the capture and  
61 accumulation of deleterious mutations can make heterozygotes more fit because they do not express this  
62 recessive genetic load leading to associative overdominance that prevents the inversion from becoming fixed  
63 [4, 11]. Capture of recessive deleterious variants within the inversion would not have an effect while the  
64 inversion is rare, because homozygotes would be very rare, but may influence its persistence as a  
65 polymorphism once it rises in frequency when the cost of reduced fitness of homozygotes is experienced [4].  
66

67 Although suppressed recombination causing tight linkage among adaptive variants located within inversions  
68 is thought to be central to their potential to develop into supergenes, inversions can also cause large  
69 effect mutations at their breakpoints. Breakpoint mutations can disrupt the coding sequence of genes (e.g.  
70 [5, 8]) or cause large deletions [2, 7]. These mutations can directly drive the phenotypic effects and be the  
71 target of selection themselves, or they can influence the evolutionary dynamics of the inversion, e.g. through  
72 recessive lethality of inversion homozygotes [5, 8]. Alternatively, selection may act on an adaptive breakpoint  
73 in combination with adaptive variants within the inversion, or in regions of reduced recombination extending  
74 beyond the breakpoints [7], to which they are linked. Unlike the variants contained within the inversion,  
75 breakpoint mutations occur concurrently with the inversion and so naturally segregate perfectly with it.  
76 However, because inversion breakpoints are often highly repetitive, they have been difficult to assemble and  
77 characterize using short-read sequencing and, consequently, our understanding of their contribution to  
78 supergene formation is incomplete [7].  
79

80 Atlantic salmon (*Salmo salar*) is an anadromous fish that spends its juvenile period in freshwater before  
81 undergoing a marine feeding migration and then returning to freshwater to spawn. Natal homing promotes  
82 local adaptation among heterogenous riverine environments [14]. Imperfect homing can lead to gene flow  
83 among these locally adapted populations that can promote the recruitment of large-effect loci [15]. These  
84 conditions are likely to favor inversion polymorphisms as shown in other salmonids (e.g. rainbow trout [3]).  
85 Salmonids experienced a whole-genome duplication (WGD) event 85-106 million years ago from which many  
86 duplicate genes are retained [16]. Large chromosomal rearrangements have been an important evolutionary  
87 mechanism during rediploidization following the WGD [16], but the present polymorphic inversion landscape  
88 in Atlantic salmon remains poorly characterized.  
89

90 Despite phenomenal advances in the detection and characterization of inversions, challenges remain  
91 regarding characterizing of inversion breakpoints, especially those containing inverted repeats or segmental  
92 duplications [7]. Here we identified polymorphic inversions using newly available long-read assemblies from  
93 11 Atlantic salmon sampled across the species range, representing all four phylogeographic groups; North  
94 American (NAm), Baltic (BAL), Barents/White Sea (BWS) and Atlantic (ATL) [17]. We systematically searched  
95 the Atlantic salmon genome for inversions using assembly-based detection and investigated their potential  
96 for supergene formation. Long-read sequencing of its sister species, brown trout (*Salmo trutta*), was used to  
97 determine the standard arrangement of the inversions and characterize breakpoints. We use these  
98 inversions to investigate the importance of the capture of preexisting variation for supergene emergence.  
99

## 100 **Material and Methods**

### 101 *Nanopore long-read sequencing and building of genome assemblies*

102 The Atlantic salmon reference genome (GCA\_905237065.2) was built from 70x genome coverage with long-  
103 read Oxford Nanopore reads generated from a Norwegian aquaculture salmon (AQGE; Table S1). Long-read  
104 libraries were prepared using the SQK-LSK109 kit following the Genomic DNA by ligation protocol and  
105 sequenced on a PromethION sequencer. Initially, five *de novo* assemblies were generated with varying  
106 sequence overlaps (5, 10, 15, 20 and 30kb) using Flye v2.7 and v2.8 [18]. Contigs from the five assemblies  
107 were combined into one assembly by merging contig ends overlapping with >20kb or more determined from

108 LASTZ alignments [19]. The combined assembly was polished with long-reads using PEPPER (v0.0.6) [20] and  
109 Illumina short-reads using pilon (v1.23) [21]. Hi-C data was used to build chromosome sequences. Except for  
110 Hi-C, the assembly pipeline described above was used to create 10 additional genome assemblies for Atlantic  
111 salmon, as well as the brown trout assembly used for determining the standard arrangement of the  
112 inversions (Table S1).

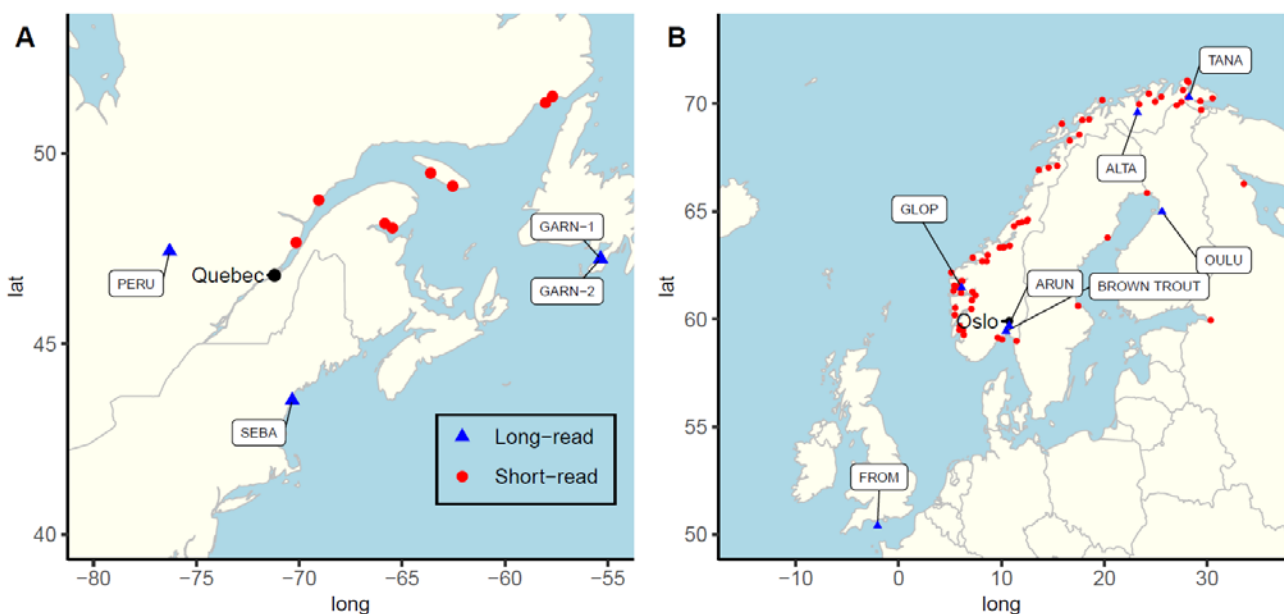
### 113 114 *Inversion detection*

115 We detected inversions in the long-read sequenced samples with both read-mapping and assembly  
116 comparisons. For the read-based SV-calling pipeline, see electronic supplementary material. Custom scripts  
117 can be found at [https://github.com/kristinastenklokk/long\\_read\\_SV](https://github.com/kristinastenklokk/long_read_SV). Assembly alignments were made with  
118 Minimap2 v2.23 [22] and were used to verify the candidate inversions from the read-based SV-detection  
119 pipeline, limited to inversions  $\geq 10$ kb that are visible in assembly alignments, and to detect additional large  
120 inversions that read-based methods have low power to detect. This provided a set of 11 high confidence  
121 inversions (for details see Data S1). For inspection of repeat blocks in inversion breakpoints, we created self-  
122 alignments with LASTZ v1.0.4 [19], (Figure S1). These 11 inversions were genotyped by manual inspection of  
123 plots where contigs and nanopore reads were mapped to inversion breakpoints using Minimap2 v2.23 [22].  
124 To validate heterozygous inversions in the reference AQGE, ultra-long reads were created with PromethION  
125 using the Ultra-Long DNA Sequencing Kit and protocol (SQK-ULK001, v.ULK\_9124\_v110\_revA\_24Mar2021).  
126 Figure S2B demonstrates how a AQGE ultra-long read mapped to the AQGE assembly reveals that both  
127 orientations of the inversion are present and resolving that AQGE is heterozygous for the inversion. Figure  
128 S2C shows mapping of a contig from the OULU assembly spanning the repeat structure of the upstream  
129 inversion breakpoint of chr9inv, validating the alternative state of the inversion in this sample.

### 130 131 *Illumina short-read mapping and variant calling*

132 For the short-read mapping and variant calling we used Illumina data from the whole genome re-sequencing  
133 of 482 Atlantic salmon sampled from a broad phylogeographic distribution [23] (Figure 1, Data S2). The  
134 Illumina reads were mapped to the Atlantic salmon genome (Ssal\_v3.1; GCA\_905237065.2) using the bcbio-  
135 nextgen v1.2.3 pipeline [24] with the bwa-mem aligner v.0.7.17 [25]. Aligned reads were sorted with  
136 Samtools v1.9 [26] and duplicate reads were marked with Sambamba v0.7.1 [27]. Genomic variation was  
137 identified using Google's DeepVariant pipeline v1.1.2 with default parameters [28] and the individual  
138 genotypes were merged using Glnexus v1.2.2 with the 'DeepVariantWGS' configuration [29]. Variants were  
139 then filtered for depth  $>4$  and  $<40$ , genotype quality  $>10$  followed by missingness  $<30\%$  in vcftools (v0.1.16).

140  
141



142  
143 **Figure 1: Map of sampling sites.** Location of wild Atlantic salmon and brown trout samples used in study. Blue triangles designate  
144 nanopore long-read sequenced samples used for inversion detection and red dots indicate populations sampled and sequenced with  
145 Illumina short-read in North America (A) and Europe (B).

146  
147  
148  
149  
150  
151  
152  
153  
154  
155  
156  
157  
158  
159  
160  
161  
162  
163  
164  
165  
166  
167  
168  
169  
170  
171  
172  
173  
174  
175  
176  
177  
178  
179  
180  
181  
182  
183  
184  
185  
186  
187  
188  
189  
190  
191  
192  
193  
194  
195  
196  
197

### *Identifying tag-SNPs and inversions type in population samples*

To identify SNPs ‘tagging’ the standard and inverted haplotypes we used Illumina short-read genotype data for the same individuals as were genotyped using long-read data (Table S1). This comparison allowed us to validate the ability of the short-read data to correctly call inversion genotypes as determined from long-read assembly comparisons (see above). Haplotypes were determined separately for Europe and North America as there is strong genetic structure between the continents that is not linked to the inversion. No haplotype structure was determined for chr16inv because no short-read SNPs were called in this short (~77kb) inversion. To phase inversions variants and SNPs we used Princess v0.01 [30] with default parameters. After phasing, unphased loci were removed, and SNPs and inversion variants were refined and merged using Jasmine v1.1.0 [31]. Exemplified by chr18inv, a total of 146 SNPs, which perfectly match inversion types in the 11 long-read samples, were defined as tag-SNPs and used to genotype eight populations in North America using the short-read data (Figure 2A). Scripts can be found at [https://github.com/mariesaitou/supergenes\\_inversions](https://github.com/mariesaitou/supergenes_inversions).

### *Inversion dating*

For inversions with inversion-linked haplotype structure and length greater than 100kb (~1cM) (Data S1), we dated the inversions using the split function in smc++ v1.15.2 [32]. We used alternate homozygotes as defined from the haplotype analysis (Figure 2B, Figure S3), i.e. standard and inverted homozygotes, as populations and SNPs within the inverted region. These conditions were only met for chr18inv in North America (n=41 standard and 21 inverted homozygotes). A mutation rate of  $1.06 \times 10^{-8}$  was inferred by comparing sequence divergence between long-read sequenced individuals from Europe and North America and an estimated divergence time of 0.5MY [33].

### *Genotype-Environment associations*

To test if inversions were associated with adaptive variation, we tested for genotype-environment associations (GEA) determined using the Latent Factor Mixed Model (LFMM) approach [34] in the R package lea (R v4.1)[35]. LFMM fits a linear mixed-model with population structure controlled simultaneously to model estimation using latent factors, where the expected number of genetic clusters (K) is the latent factor, which was estimated using admixture (v1.23) [36]. Environment associations were tested on the pooled European (n=402) and the North American (n=80) samples separately because the strong differentiation between these lineages would confound associations and some inversions were only polymorphic in one group. Environment associations were tested for all SNPs on chromosomes containing an inversion (8 chromosomes, 1.07-1.23 million SNPs). False discovery control was employed using the Benjamini–Hochberg procedure with alpha thresholds of 0.05 and 0.01 across all tests. Variants were phased and imputed using Beagle v5.2 [37] (burnin 3, interactions 12, phase states 280) and then filtered for minor allele frequency >5%. Environment variables tested related to thermal, precipitation and river size conditions in the spawning and juvenile habitat expected to exert selection pressures on salmon. The individual river parameters were obtained from the WorldClim database for an arc of 30 translating to 1 square km at the river mouth (<https://www.worldclim.org>) to ensure comparable data quality and availability for all rivers. Air temperature has been shown to represent water temperature in Norway except at low temperatures [38], likely because winter ice cover in some rivers can lead to discrepancies in air and water temperatures. Annual temperature, and additionally the temperature in the coldest and warmest quarters, were selected as these influence the overwinter survival and growth potential respectively. Inversions were inferred to have adaptive potential where they overlap with multiple variant associations suggesting that the inversion has the potential to link different adaptive variants and is capable of becoming a supergene. The frequency of associated loci was calculated for inversion homozygotes, to avoid any influence of phasing errors, by summing the allele count and dividing by twice the number of homozygous individuals for each arrangement.

### *Mutation load*

To test for the accumulation of deleterious mutations we predicted missense variants with snpEff v5.0e [39] on variant calls (filtered with vcftools v0.1.16 on minor allele count = 2). PROVEAN scores (PROVEAN v1.1.5

198 [40]) were computed to assess the impact of the detected missense variants for each protein using the  
199 Ensembl Rapid Release annotation of GCA\_905237065.2. PROVEAN scores  $\geq |2.5|$  were defined as  
200 deleterious. We compared the density of deleterious mutations within inversions to the genome wide level  
201 by dividing the number of significant PROVEAN scores by the number of genes per megabase (Mb) to obtain  
202 the mutation load per gene and Mb. We used the Wilcoxon Rank Sum test to test for significant enrichment  
203 inside inversions.

204

#### 205 *Detection of indels within inversions*

206 Indels were called using the long-read based detection pipeline (electronic supplementary material,  
207 Methods). Insertions and deletions were filtered based on length using a common minimum cut-off of 50bp  
208 and a maximum of 100kb, as earlier studies have shown that it is challenging to reliably call longer insertions  
209 [30]. To assess indel enrichment within inversions, we compared the indel density inside inversions by indel  
210 densities within corresponding homeologous regions in the Atlantic salmon genome. Indel density was  
211 calculated as the number of indels per sequence length.

212

## 213 **Results and Discussion**

### 214 *Detection and characterization of inversions*

215 Long-read data from 11 Atlantic salmon sampled across the species' range were used to systematically  
216 identify inversions, allowing us to detect and compare inversions that had not formed supergenes to those  
217 with supergene characteristics. Read-based methods for structural variant detection had low precision  
218 regarding the position and size of the inversions, indicating a high number of false positives. These  
219 inconsistencies are likely because of the complex breakpoint repeat structures as the only large inversion  
220 detected by these methods had simple non-repetitive breakpoints (chr18inv). In contrast, assembly-based  
221 methods were much more reliable for detecting and genotyping inversions. Assembly methods detected a  
222 modest but reliable set of 11 inversions, with five inversions being larger than 1.5 Mb and containing multiple  
223 genes (summarized in Data S1). All inversions detected by the method were observed in more than one  
224 individual corroborating that the inversions are real and polymorphic. The increasing availability of multiple  
225 assemblies (pangenomes) will facilitate the detection of inversions by this method in more species.

226 Further, alignment of chromosome sequences in the Atlantic salmon reference (AQGE; GCA\_905237065.2)  
227 with syntenic regions in the sister species brown trout, shows that for chr4inv, chr11inv3, chr16inv, chr18inv,  
228 chr22inv and chr26inv the reference has the standard configuration, whereas for chr3inv, chr9inv, chr10inv,  
229 chr11inv1 and chr11inv2 it has the inverted orientation (Figure S4).

230

### 231 *Characterization of inversion breakpoints*

232 Inversion breakpoints can have functional impacts, e.g. by disrupting coding genes, and can impact the  
233 evolution of inversions, but can be difficult to sequence through as they are often highly repetitive. To  
234 characterize inversion breakpoints, we analyzed both nanopore reads and multiple *de novo* assemblies of  
235 the 11 Atlantic salmon (Table S1). Five inversions (chr3inv, chr9inv, chr11inv3, chr22inv and chr26inv) are  
236 flanked by complex tandem repeats, four of which (chr3inv, chr9inv, chr22inv and chr26inv), have similar  
237 tandem motifs at both breakpoints (see Figure S1). Shared repeat expansions on either end of these  
238 inversions may indicate recurrence and may make the development of a supergene less likely by permitting  
239 recombination among haplotypes. chr18inv is the only large, multigene inversion with no obvious repeat  
240 structures at the inversion breakpoints (Figure S1-H). For the large inversions with matched tandem repeats  
241 at both breakpoints we were unable to detect extended LD and the development of divergent haplotypes,  
242 suggesting they are younger or recurrent inversions that may be unlikely to become supergenes. While the  
243 small chr3inv did have haplotype structure, this did not reflect the inversion genotype and so probably  
244 reflects the small size of the region.

245

246 Three of the inversions have possible functional impacts through gene-disrupting breakpoints. The upstream  
247 breakpoint of chr18inv breaks in intron 1 of *MRC2-like* (Figure 3C), making the gene likely to become non-  
248 functional. Mannose receptor genes have immune-related functions and have been shown to be upregulated  
249 following bacterial infection in fish [41]. Two copies of *MRC2-like* are found nearby that may compensate for  
250 the breakpoint mutation, preventing negative fitness effects (Figure S5). Chr22inv disrupts genes at both  
251 breakpoints, breaking *TGM2-like* and *VRK3* at the upstream (Figure S6A) and *DNASE1L3* at the downstream

252 breakpoint (Figure S6B). *TGM2* is involved in cell death, pro-inflammatory response [42] and is associated  
253 with the environment in Arctic Charr [43]. *VRK3* is also involved in apoptosis and inflammatory processes  
254 [44]. *DNASE1L3* is known to mediate degradation of DNA during apoptosis [45]. We observed individuals  
255 homozygous for the gene breaks for chr18inv and chr22inv, implying that they are not lethal, as observed for  
256 some inversion supergenes (e.g. [5, 8]). Finally, the downstream breakpoint of chr26inv disrupts  
257 *BAT1/DDX39B* (Figure S7), a helicase involved in RNA metabolism and inflammatory disease [46].  
258 Duplications are present at both the upstream (~300kb; pos. 52,003,636-52,306,925) and downstream  
259 (~100kb; pos. 53,816,770-53,913,337) breakpoints of chr26inv (Figure S1 J), however, no protein-coding  
260 genes are duplicated and so the functional consequences are unclear. Negative effects of breakpoint-induced  
261 gene disruptions may prevent these inversions from successfully spreading. However, many genes in the  
262 Atlantic salmon genome have functional duplicates originating from the salmonid whole genome duplication,  
263 which may compensate for eventual functional consequences of some of these gene disruptions.

264

#### 265 *Accumulation of deleterious mutations and indel enrichment*

266 Recombination suppression makes inversions vulnerable to the accumulation of deleterious mutations,  
267 which could be important in determining their fate. If recessive deleterious mutations accumulate it can  
268 result in associative overdominance, where heterozygous individuals are more fit [2, 4, 10]. None of the  
269 inversions showed significant enrichment of deleterious mutations (Wilcoxon Rank Sum test;  $P > 0.05$ ) (Figure  
270 S8). For three of the inversions (chr3inv, chr18inv and chr26inv) there is a >2x enrichment of small indels  
271 compared to their corresponding homeologous region in the salmon genome (Table S2). One 260 bp deletion,  
272 fixed in the standard chr18inv arrangement in North American populations, overlaps the 3'-end of *P2RY5*  
273 (*P2Y* purinoceptor 5; ENSSSAG00000044266), indicating that it may be of functional importance (Figure S9).  
274 However, for chr18inv there is no evidence for a deleterious impact of inversion homozygosity, since both  
275 haplotypes were frequent in our population samples. These results suggest that it may be too early in the  
276 evolution of chr18inv for sufficient deleterious mutations to have accumulated to influence the maintenance  
277 of the inversion.

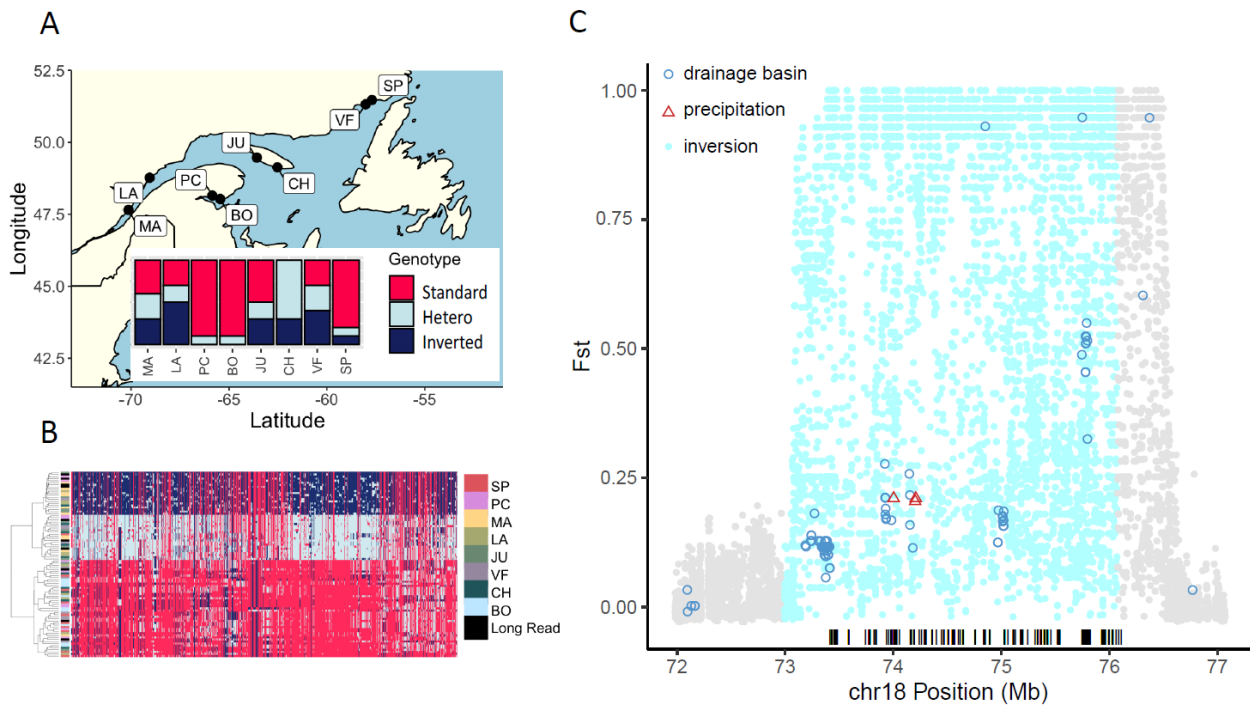
278

#### 279 *Haplotype structure within inversions*

280 A key aspect of supergene formation and invasion is reduced recombination leading to strong linkage  
281 disequilibrium (LD) and divergent haplotypes. Only six inversions have haplotype structures extending across  
282 the inversion: chr3inv, chr11inv2, chr11inv3 and chr18inv in North America, and chr4inv and chr11inv1 in  
283 Europe (Figure S3). However, only for chr4inv and chr18inv did this structure match the inversion genotype  
284 from long-read analyses (Data S3). This suggests that the other inversions are either recurrent, so little  
285 structure has developed, or rare such that the haplotypes are dominated by one configuration. The large  
286 multigene chr18inv inversion is frequent (0.38) across eight North American populations (Figure 2A) and the  
287 short chr4inv was also frequent in Europe (0.31). Consistent with the clear haplotype structure,  $F_{ST}$  between  
288 alternative homozygotes for chr18inv was strongly elevated across the inversion (Figure 2C). The elevation  
289 of  $F_{ST}$  extends beyond the downstream breakpoint, suggesting that recombination is also suppressed for  
290 ~490kb downstream of the inversion. We found no indication in the long-read assemblies for further linked  
291 structural variants that could explain this extended recombination suppression, but such may be present in  
292 other individuals.

293

294



295  
 296 **Figure 2. Chr18inv haplotype structure and  $F_{ST}$  between inverted and standard arrangements.** A. Location of samples and estimated  
 297 chr18inv haplotype frequencies in different Canadian rivers based on short-read sequence data. BO: Bonaventure, CH,  
 298 De\_la\_Chaloupe, JU: Jupiter, LA: Laval, MA: Malbaie\_(Charlevoix), PC: Petite\_riviere\_Cascapedia, SP: Saint-Paul, VF, Du\_Vieux\_Fort.  
 299 B. Red: reference homozygous type, Light blue: heterozygous type, Navy blue: inversion homozygous type. B. Haplotype structure  
 300 within the chr18inv region (The 1000th to the 2000th variants were selected from the 4828 variants to reduce the computational load  
 301 for the effective visualization) based on short-read sequence data in North American populations. Individuals with long-read  
 302 sequences are highlighted in black in the left bar. The haplotype structure of the entire inversion is described in Figure S3. C.  $F_{ST}$  (Weir  
 303 and Cockerham) between homozygotes with alternative inversion orientations showing environment associated SNPs with  $p < 0.05$ ,  
 304 black bars under plot show the positions of tag-SNPs used to genotype the inversion.  
 305

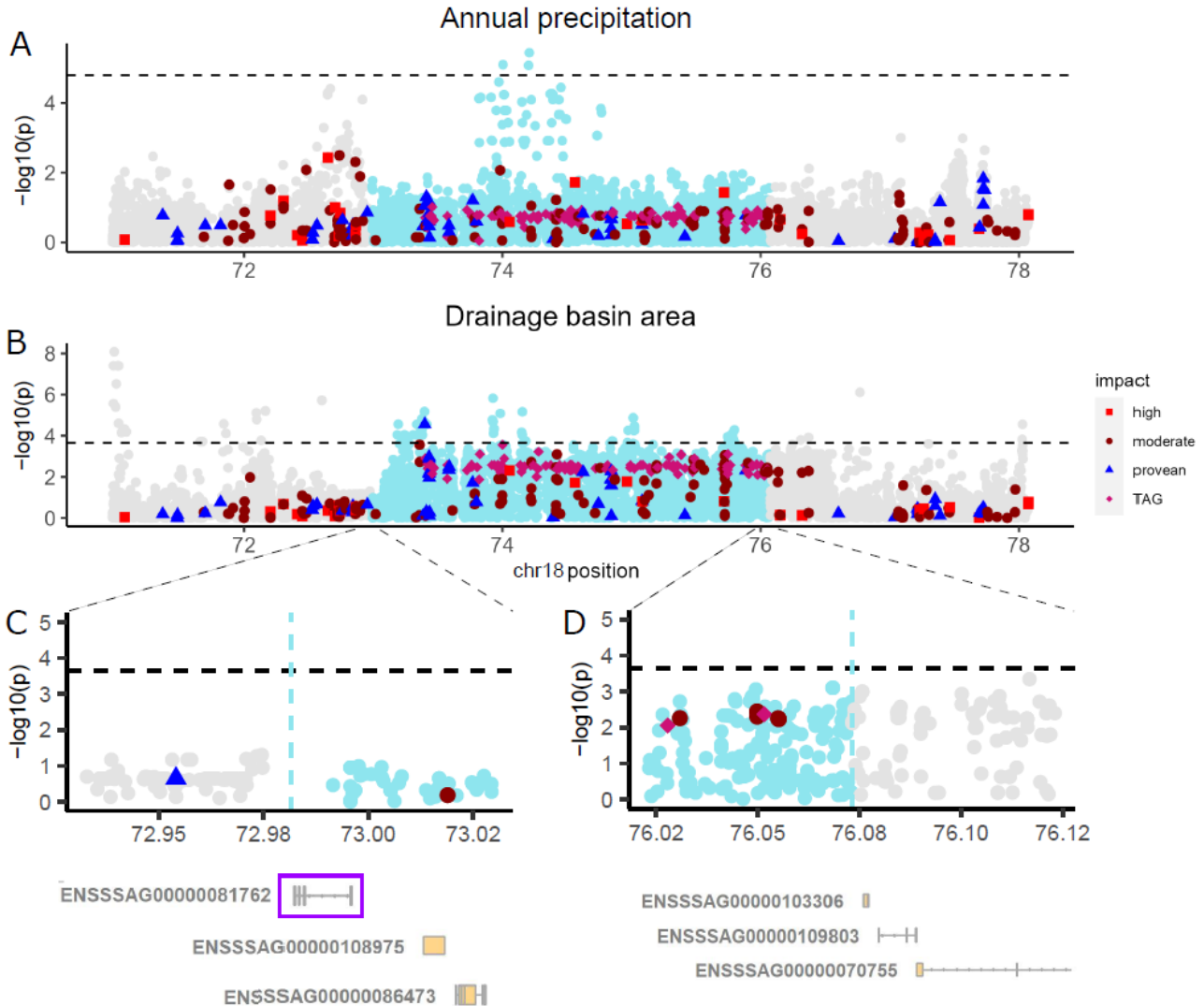
### 306 *Dating of the inversions*

307 Only one inversion could be dated because it had inversion-linked haplotype structure and was  $>100\text{kb}$ , i.e.  
 308  $>\sim 1\text{cM}$ . The chr18inv inversion was estimated to have split from the standard arrangement  $\sim 5000$   
 309 generations,  $\sim 15,000$  years ago (Figure S10) making this a young inversion, originating about the time of the  
 310 last glacial retreat.

### 312 *Genotype-environment associations*

313 Local adaptation with gene flow, as occurs in Atlantic salmon, has been suggested as a driver for the  
 314 establishment of inversions because recombination suppression within the inversion can protect locally co-  
 315 adapted variants from being broken apart by the influx of migrant variation [10, 12]. To become a supergene  
 316 the region of suppressed recombination should link together multiple adaptive variants that behave as a  
 317 single haplotype[1]. Larger inversions are expected to capture more genes and locally adapted alleles, which  
 318 may help to explain their greater likelihood of being recruited as supergenes [10]. Consistent with this  
 319 prediction, among 11 inversions only four large ( $>1.5\text{Mb}$ ) multigene inversions (Data S1) overlapped with  
 320 environment association peaks, three of which overlapped with multiple environments. Chr9inv and chr26inv  
 321 have associations with two different environments in Europe and chr9inv with three in North America (Figure  
 322 S11), which were weak to moderately correlated ( $r^2 = 0.01-0.43$  Table S3). Chr18inv is only polymorphic in  
 323 North America where multiple associations were found with two environmental variables, annual mean  
 324 precipitation (LFMM  $p < 0.05$ ) and drainage basin area (LFMM  $p < 0.05$ ) (see Figure 3, Figure S11a, S11c),  
 325 which are weakly correlated ( $r^2 = 0.17$ , Table S3). None of the associations overlapped the breakpoints,  
 326 suggesting these are not involved in environmental adaptation to these variables. Further work will be  
 327 required to determine if the gene disrupting breakpoint is adaptive, or just tolerated. These results suggest  
 328 that the potential for large inversions to capture and link adaptive clusters is common, in line with

329 expectations [47]. However, only chr18inv had both environment associations and a strong inversion-linked  
 330 haplotype structure (Figure 11c, Figure S3), indicative of supergene formation, suggesting the presence of  
 331 pre-existing adaptive variation is not sufficient alone or favorable allele combinations were not captured in  
 332 the three other inversions.  
 333  
 334  
 335



336  
 337 **Figure 3. Genotype-environment associations for chr18inv.** Associations with **A** annual precipitation and **B** drainage basin area,  
 338 functional- and tag-SNPs are highlighted for the inversion (blue) and 2Mb flanking (grey). Significant associations, dashed horizontal  
 339 line, indicates significance level  $p < 0.05$ . Red squares (high) and dark red points (moderate) show functional impact estimated by  
 340 SNPEff on protein-coding genes. Blue triangles show significant deleterious mutations estimated by PROVEAN, whereas pink  
 341 diamonds represent tag-SNPs for chr18inv. Zoom-in of breakpoints **C** and **D** show one gene (*MRC2-like*, ENSSSAG00000081762)  
 342 overlapping breakpoint at ~72.98Mb (purple frame).  
 343

344 *Capture and accumulation of adaptive variation*

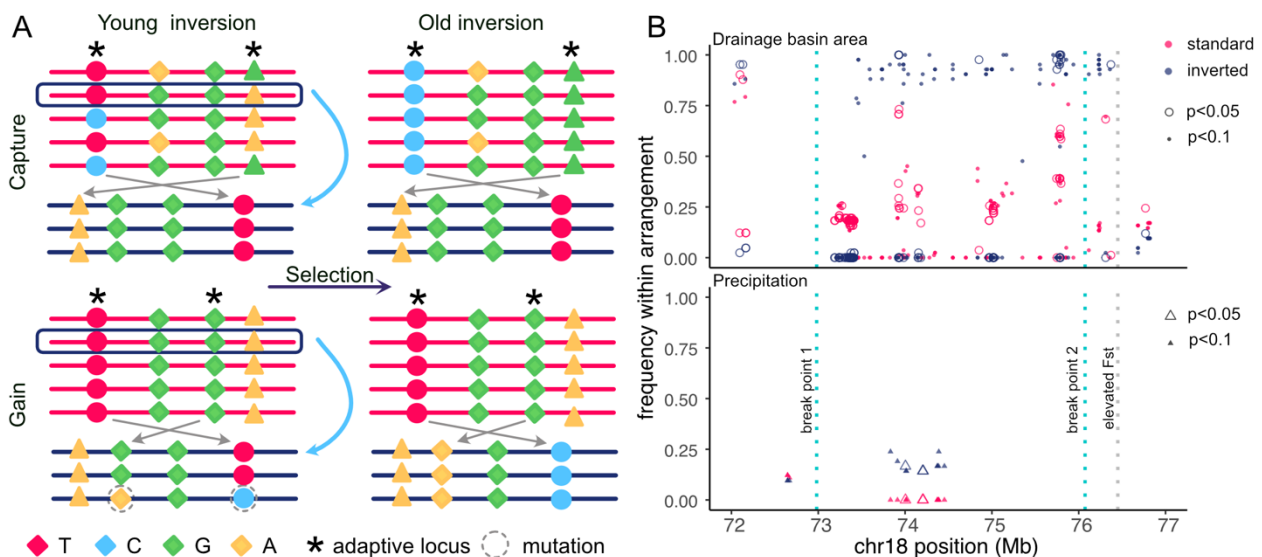
345 Whether environment associations arise from the capture of pre-existing variation and, therefore, are  
 346 important in establishing the inversion, or accumulate over time after inversions have occurred, is still  
 347 unclear [6, 12, 13, 47]. When an inversion is first formed it is expected that the inverted arrangement will be  
 348 invariant, having captured a single standard haplotype (Figure 4A). In contrast, initially the standard  
 349 arrangement will still carry any allelic variation that was previously segregating in the population, including  
 350 that captured by the inversion [10]. Over time, this variation will be lost by drift and selection in the standard  
 351 arrangement and the inverted arrangement haplotypes will gain variation via new mutations [10] (Figure 4A).  
 352 For the inversion to be maintained the linkage among adaptive variants within the inverted arrangement  
 353 should confer higher fitness than the same variants within the recombining standard arrangement. Only  
 354 three significant variants were found to be strongly differentiated (LFMM  $p < 0.05$  and  $F_{st} > 0.8$ ) across



355 chr18inv (Figure 2C), one of which is located outside of the inverted region, but within the area of suppressed  
 356 recombination downstream of the distal breakpoint. The inverted arrangement is fixed or nearly fixed for all  
 357 alleles associated with drainage basin area at  $p < 0.05$ , while in the standard arrangement these alleles have  
 358 intermediate frequencies (Figure 4B). This pattern explains the elevated but moderate  $F_{st}$ s for most adaptive  
 359 variants (Figure 2C) and is consistent with retention of pre-existing adaptive polymorphisms in a young  
 360 inversion. The pattern is less strong for weakly associated SNPs,  $p < 0.1$ , where three SNPs had intermediate  
 361 frequencies in the inverted arrangement. The pattern is reversed for precipitation associated SNPs, all of  
 362 which are fixed in the standard arrangement but are variable in the inverted arrangement, suggesting that  
 363 sufficient time has elapsed since the inversion event to allow the generation of new adaptive variation in the  
 364 inverted arrangement (Figure 4B). These patterns suggest that the inversion has captured previously  
 365 segregating adaptive polymorphisms, linking them within the inversion, but selection and drift have not yet  
 366 removed the pre-existing variation within the standard arrangement. However, at least some adaptive  
 367 variation has emerged within the inverted arrangement.

369 The inversion remains polymorphic in all populations (Figure 2A), co-existence of both arrangements is  
 370 expected if the migration rate is not so high that it leads to swamping. The maximum benefit of an inversion  
 371 is expected when migration is just below this critical level [12]. If the spatial heterogeneity occurs over small  
 372 scales, or environmental variation is continuous we also expect within population inversion polymorphisms  
 373 to persist. All these factors are likely to contribute to the maintenance of within population polymorphism  
 374 here. Lee et al. (2017) [6], also found support for capture in a young inversion (~2.1-8.8ka) in a relative of  
 375 *Arabidopsis*. However, because high levels of self-fertilization would reduce the benefit of recombination  
 376 suppression, invasion of a supergene by this mechanism was difficult to reconcile with model expectations  
 377 [12]. Here we find evidence for capture and accumulation of adaptive variation in an outcrossed species  
 378 where populations are connected by gene flow. Both capture of pre-existing and subsequent accumulation  
 379 of adaptive variation is also suggested for a butterfly mimicry supergene in analysis presented by Jay et al in  
 380 this special issue [13].

381  
 382



383  
 384 **Figure 4. Capture and accumulation of adaptive variation by inversions.** A. When an inversion first occurs the inverted arrangement  
 385 captures a single invariant haplotype, while the standard arrangement will still have multiple variable haplotypes including pre-  
 386 existing adaptive variation (upper left). Following the inversion event, the inverted arrangement may accumulate new adaptive  
 387 mutations that are not present in the standard arrangement (lower left). Over time selection for alternatively coadapted allelic  
 388 combinations results in the fixation of adaptive variation in the standard arrangement (upper right) and selective sweeps and fixation  
 389 of adaptive new mutations in the inverted arrangement (lower right) making the origin of the variation hard to determine. B.  
 390 Frequency of environment-associated SNPs (LFMM open symbols  $p < 0.05$ , closed symbols  $p < 0.1$  circles: drainage basin, triangles:  
 391 precipitation) in standard and inverted homozygotes pooled across eight North American populations. Drainage basin associated  
 392 SNPs are almost all fixed or nearly fixed in the inverted arrangement, especially for  $p < 0.05$ , as expected for a young inversion, whereas  
 393 most variants segregate at intermediate frequencies in the standard arrangement. Only three SNPs were nearly fixed for alternative  
 394 alleles between standard and inverted arrangements, a pattern expected to occur in older inversions. In contrast, precipitation  
 395 associated SNPs are fixed in the standard arrangement, suggesting variation in the inverted arrangement has accumulated since the  
 396 inversion occurred.

397  
398  
399  
400  
401  
402  
403  
404  
405  
406  
407  
408  
409  
410  
411  
412  
413  
414  
415  
416  
417  
418  
419  
420  
421  
422  
423  
424  
425  
426  
427  
428  
429  
430  
431  
432  
433  
434  
435  
436  
437  
438  
439  
440  
441  
442  
443  
444  
445  
446  
447  
448  
449

## Conclusions

Our genome wide survey of inversions in Atlantic salmon detected 11 highly reliable inversions. Of these, two showed evidence of inversion driven haplotype formation. Only large multigene inversions overlapped with adaptive variants as detected by GEA, and among these only chr18inv also had inversion-linked haplotype structure. For chr18inv we found evidence that the adaptive variants linked to the inverted haplotype also segregate as ancestral polymorphisms as they are still present in the standard arrangement haplotypes. Additionally, adaptive variation has accumulated within the inverted haplotype since its formation. These findings support that both the capture of preexisting variation and subsequent accumulation of variation has been important in forming this emerging supergene. Three of the 11 inversions had breakpoints that disrupted genes. For chr18inv, the disruption could be compensated for by local duplicates. Our results suggest that multiple processes contribute to the formation of supergenes from inversions, e.g. both capture and accumulation of adaptive variation and tolerated breakpoint mutations, but do not support an early role for deleterious mutation load.

## Data availability

Illumina whole-genome sequencing data of 482 individuals are available in projects (PRJEB38061). The long-read genome assemblies have been submitted to ENA, project accessions listed in Table S1. Environmental information for the environment associations is contained in Data S2. The authors declare that all data supporting the findings of this study are available within the paper and its electronic supplementary material [48].

Authors' contributions. K.S.: data curation, formal analysis, investigation, methodology, visualization, writing—original draft, writing—review and editing; M.S.: formal analysis, investigation, visualization, writing—original draft, writing—review and editing; L.R.-J.: formal analysis; T.N.: formal analysis, methodology, writing—review and editing; M.M.: formal analysis, methodology, writing—review and editing; M.Á.: formal analysis, methodology, writing—review and editing; M.K.: formal analysis, methodology, writing—review and editing; N.J.B.: conceptualization, data curation, formal analysis, funding acquisition, investigation, methodology, supervision, visualization, writing— original draft, writing—review and editing; S.L.: conceptualization, data curation, formal analysis, methodology, project administration, resources, supervision, writing—original draft, writing—review and editing.

All authors gave final approval for publication and agreed to be held accountable for the work performed therein.

## Acknowledgements

The study was supported by The Research Council of Norway (grant nos. 275310 and 221734).. We thank Sarah Lehnert, Ian Bradbury, Louis Bernatchez, Cooke Aquaculture Inc., AquaGen AS, Craig Primmer, Jamie Stevens, Harald Sægrov, Jenny Jensen and Thrond Haugen for providing samples for the nanopore sequencing. We acknowledge the use of the Orion computing cluster at the Norwegian University of Life Sciences (NMBU). Storage resources were provided by the Norwegian National Infrastructure for Research Data (NIRD, project NS9055K). We thank two anonymous reviewers and the editor for thoughtful comments that improved the manuscript.

## References

- [1] Thompson, M. J. & Jiggins, C. D. 2014 Supergenes and their role in evolution. *Heredity* (Edinb) 113, 1-8. (doi:10.1038/hdy.2014.20).
- [2] Gutiérrez-Valencia, J., Hughes, P. W., Berdan, E. L. & Slotte, T. 2021 The Genomic Architecture and Evolutionary Fates of Supergenes. *Genome Biology and Evolution* 13, evab057. (DOI:<https://doi.org/10.1093/gbe/evab057>).
- [3] Pearse, D. E., Barson, N. J., Nome, T., Gao, G., Campbell, M. A., Abadía-Cardoso, A., Anderson, E. C., Rundio, D. E., Williams, T. H., Naish, K. A., et al. 2019 Sex-dependent dominance maintains migration

450 supergene in rainbow trout. *Nature Ecology & Evolution* 3, 1731-1742.  
451 (DOI:<https://doi.org/10.1038/s41559-019-1044-6>).

452 [4] Jay, P., Chouteau, M., Whibley, A., Bastide, H., Parrinello, H., Llaurens, V. & Joron, M. 2021 Mutation  
453 load at a mimicry supergene sheds new light on the evolution of inversion polymorphisms. *Nature Genetics*  
454 53, 288-293. (DOI:<https://doi.org/10.1038/s41588-020-00771-1>).

455 [5] Lamichhaney, S., Fan, G., Widemo, F., Gunnarsson, U., Thalmann, D. S., Hoepfner, M. P., Kerje, S.,  
456 Gustafson, U., Shi, C., Zhang, H., et al. 2016 Structural genomic changes underlie alternative reproductive  
457 strategies in the ruff (*Philomachus pugnax*). *Nature Genetics* 48, 84-88.  
458 (DOI:<https://doi.org/10.1038/ng.3430>).

459 [6] Lee, C.-R., Wang, B., Mojica, J. P., Mandáková, T., Prasad, K. V. S. K., Goicoechea, J. L., Perera, N.,  
460 Hellsten, U., Hundley, H. N., Johnson, J., et al. 2017 Young inversion with multiple linked QTLs under  
461 selection in a hybrid zone. *Nature Ecology & Evolution* 1, 0119. (DOI:<https://doi.org/10.1038/s41559-017-0119-0119>).

462 [7] Villoutreix, R., Ayala, D., Joron, M., Gompert, Z., Feder, J. L. & Nosil, P. J. M. E. 2021 Inversion  
463 breakpoints and the evolution of supergenes. *Molecular Ecology*.  
464 (DOI:<https://doi.org/10.1111/mec.15907>).

465 [8] Küpper, C., Stocks, M., Risse, J. E., dos Remedios, N., Farrell, L. L., McRae, S. B., Morgan, T. C.,  
466 Karlionova, N., Pinchuk, P., Verkuil, Y. I., et al. 2016 A supergene determines highly divergent male  
467 reproductive morphs in the ruff. *Nature Genetics* 48, 79-83. (DOI:<https://doi.org/10.1038/ng.3443>).

468 [9] Giraldo-Deck, L. M., Loveland, J. L., Goymann, W., Tschirren, B., Burke, T., Kempnaers, B., Lank, D. B. &  
469 Küpper, C. 2022 Intralocus conflicts associated with a supergene. *Nature Communications* 13, 1384.  
470 (DOI:<https://doi.org/10.1038/s41467-022-29033-w>).

471 [10] Faria, R., Johannesson, K., Butlin, R. K. & Westram, A. M. 2019 Evolving Inversions. *Trends in Ecology &*  
472 *Evolution* 34, 239-248. (DOI:<https://doi.org/10.1016/j.tree.2018.12.005>).

473 [11] Kirkpatrick, M. & Barton, N. 2006 Chromosome Inversions, Local Adaptation and Speciation. *Genetics*  
474 173, 419-434. (DOI:<https://doi.org/10.1534/genetics.117.300572>).

475 [12] Charlesworth, B. & Barton, N. H. 2018 The Spread of an Inversion with Migration and Selection.  
476 *Genetics* 208, 377-382. (DOI:<https://doi.org/10.1534/genetics.117.300426>).

477 [13] Jay P, Leroy M, Le Poul Y, Whibley A, Arias M, Chouteau M, Joron M. 2022 Association mapping of  
478 colour variations in a butterfly provides evidences that a supergene locks together a cluster of adaptive loci.  
479 *Phil. Trans. R. Soc. B* 377, 20210193. (doi:10.1098/rstb.2021.0193)

480 [14] Hutchings, J. A. & Jones, M. E. B. 1998 Life history variation and growth rate thresholds for maturity in  
481 Atlantic salmon, *Salmo salar*. *Canadian Journal of Fisheries and Aquatic Sciences* 55, 22-47.  
482 (DOI:<https://doi.org/10.1139/d98-004>).

483 [15] Barson, N. J., Aykanat, T., Hindar, K., Baranski, M., Bolstad, G. H., Fiske, P., Jacq, C., Jensen, A. J.,  
484 Johnston, S. E., Karlsson, S., et al. 2015 Sex-dependent dominance at a single locus maintains variation in  
485 age at maturity in salmon. *Nature* 528, 405-408. (DOI:<http://dx.doi.org/10.5061/dryad.23h4q>).

486 [16] Lien, S., Koop, B. F., Sandve, S. R., Miller, J. R., Kent, M. P., Nome, T., Hvidsten, T. R., Leong, J. S.,  
487 Minkley, D. R., Zimin, A., et al. 2016 The Atlantic salmon genome provides insights into rediploidization.  
488 *Nature* 533, 200-205. (DOI:<https://doi.org/10.1038/nature17164>).

489 [17] Bourret, V., Kent, M. P., Primmer, C. R., Vasemägi, A., Karlsson, S., Hindar, K., McGinnity, P., Verspoor,  
490 E., Bernatchez, L. & Lien, S. 2013 SNP-array reveals genome-wide patterns of geographical and potential  
491 adaptive divergence across the natural range of Atlantic salmon (*Salmo salar*). *Molecular Ecology* 22, 532-  
492 551. (DOI:<https://doi.org/10.1111/mec.12003>).

493 [18] Kolmogorov, M., Yuan, J., Lin, Y. & Pevzner, P. A. J. N. b. 2019 Assembly of long, error-prone reads  
494 using repeat graphs. *Nature biotechnology* 37, 540-546. (DOI:<https://doi.org/10.1038/s41587-019-0072-8>).

495 [19] Harris, R. S. 2007 Improved pairwise alignment of genomic DNA, The Pennsylvania State University.

496 [20] Shafin, K., Pesout, T., Chang, P.-C., Nattestad, M., Kolesnikov, A., Goel, S., Baid, G., Kolmogorov, M.,  
497 Eizenga, J. M. & Miga, K. H. J. N. m. 2021 Haplotype-aware variant calling with PEPPER-Margin-DeepVariant  
498 enables high accuracy in nanopore long-reads. *Nature methods* 18, 1322-1332.  
499 (DOI:<https://doi.org/10.1038/s41592-021-01299-w>).

500 [21] Walker, B. J., Abeel, T., Shea, T., Priest, M., Abouelliel, A., Sakthikumar, S., Cuomo, C. A., Zeng, Q.,  
501 Wortman, J. & Young, S. K. J. P. o. 2014 Pilon: an integrated tool for comprehensive microbial variant

503 detection and genome assembly improvement. PLOS one 9, e112963.  
504 (DOI:<https://doi.org/10.1371/journal.pone.0112963>).

505 [22] Li, H. 2018 Minimap2: pairwise alignment for nucleotide sequences. *Bioinformatics* 34, 3094-3100.  
506 (DOI:<https://doi.org/10.1093/bioinformatics/bty191>).

507 [23] Bertolotti, A. C., Layer, R. M., Gundappa, M. K., Gallagher, M. D., Pehlivanoglu, E., Nome, T., Robledo,  
508 D., Kent, M. P., Røsæg, L. L. & Holen, M. M. J. N. c. 2020 The structural variation landscape in 492 Atlantic  
509 salmon genomes. *Nature communications* 11, 1-16. (DOI:<https://doi.org/10.1038/s41467-020-18972-x>).

510 [24] Chapman, B., Kirchner, R., Pantano, L., Naumenko, S., De Smet, M., Beltrame, L., Khotiainsteva, T.,  
511 Sytchev, I., Guimera, R. V., Kern, J., et al. 2021 bcbio/bcbio-nextgen: (v1.2.9). (Zenodo).

512 [25] Li, H. 2013 Aligning sequence reads, clone sequences and assembly contigs with BWA-MEM. arXiv.

513 [26] Li, H., Handsaker, B., Wysoker, A., Fennell, T., Ruan, J., Homer, N., Marth, G., Abecasis, G. & Durbin, R.  
514 J. B. 2009 The sequence alignment/map format and SAMtools. *Bioinformatics* 25, 2078-2079.  
515 (DOI:<https://doi.org/10.1093/bioinformatics/btp352>).

516 [27] Tarasov, A., Vilella, A. J., Cuppen, E., Nijman, I. J. & Prins, P. J. B. 2015 Sambamba: fast processing of  
517 NGS alignment formats. *Bioinformatics* 31, 2032-2034.  
518 (DOI:<https://doi.org/10.1093/bioinformatics/btv098>).

519 [28] Poplin, R., Chang, P.-C., Alexander, D., Schwartz, S., Colthurst, T., Ku, A., Newburger, D., Dijamco, J.,  
520 Nguyen, N. & Afshar, P. T. J. N. b. 2018 A universal SNP and small-indel variant caller using deep neural  
521 networks. *Nature biotechnology* 36, 983-987. (DOI:<https://doi.org/10.1038/nbt.4235>).

522 [29] Yun, T., Li, H., Chang, P.-C., Lin, M. F., Carroll, A. & McLean, C. Y. J. B. 2020 Accurate, scalable cohort  
523 variant calls using DeepVariant and GLnexus. *Bioinformatics* 36, 5582-5589.  
524 (DOI:<https://doi.org/10.1093/bioinformatics/btaa1081>).

525 [30] Mahmoud, M., Doddapaneni, H., Timp, W. & Sedlazeck, F. J. J. G. b. 2021 PRINCESS: comprehensive  
526 detection of haplotype resolved SNVs, SVs, and methylation. *Genome biology* 22, 1-17.  
527 (DOI:<https://doi.org/10.1186/s13059-021-02486-w>).

528 [31] Kirsche, M., Prabhu, G., Sherman, R., Ni, B., Aganezov, S. & Schatz, M. C. J. B. 2021 Jasmine:  
529 Population-scale structural variant comparison and analysis. bioRxiv.  
530 (DOI:<https://doi.org/10.1101/2021.05.27.445886>).

531 [32] Terhorst, J., Kamm, J. A. & Song, Y. S. 2017 Robust and scalable inference of population history from  
532 hundreds of unphased whole genomes. *Nature Genetics* 49, 303-309.  
533 (DOI:<https://doi.org/10.1038/ng.3748>).

534 [33] King, T. L., Verspoor, E., Spidle, A. P., Gross, R., Phillips, R. B., Koljonen, M. L., Sanchez, J. A. & Morrison,  
535 C. L. 2007 Biodiversity and Population Structure. *The Atlantic Salmon*, 117-166.  
536 (DOI:<https://doi.org/10.1002/9780470995846.ch5>).

537 [34] Frichot, E., Schoville, S. D., Bouchard, G. & François, O. 2013 Testing for associations between loci and  
538 environmental gradients using latent factor mixed models. *Molecular biology and evolution* 30, 1687-1699.  
539 (DOI:<https://doi.org/10.1093/molbev/mst063>).

540 [35] Frichot, E. & François, O. 2015 LEA: An R package for landscape and ecological association studies.  
541 *Methods in Ecology and Evolution* 6, 925-929. (DOI:<https://doi.org/10.1111/2041-210X.12382>).

542 [36] Alexander, D. H., Novembre, J. & Lange, K. 2009 Fast model-based estimation of ancestry in unrelated  
543 individuals. *Genome research* 19, 1655-1664. (DOI:<https://doi.org/10.1101/gr.094052.109>).

544 [37] Browning, B. L., Tian, X., Zhou, Y. & Browning, S. R. J. T. A. J. o. H. G. 2021 Fast two-stage phasing of  
545 large-scale sequence data. *The American Journal of Human Genetics* 108, 1880-1890.  
546 (DOI:<https://doi.org/10.1016/j.ajhg.2021.08.005>).

547 [38] Otero, J., L'Abée-Lund, J. H., Castro-Santos, T., Leonardsson, K., Storvik, G. O., Jonsson, B., Dempson, B.,  
548 Russell, I. C., Jensen, A. J., Baglinière, J.-L., et al. 2014 Basin-scale phenology and effects of climate  
549 variability on global timing of initial seaward migration of Atlantic salmon (*Salmo salar*). *Global Change*  
550 *Biology* 20, 61-75. (DOI:<https://doi.org/10.1111/gcb.12363>).

551 [39] Cingolani, P., Platts, A., Wang, L. L., Coon, M., Nguyen, T., Wang, L., Land, S. J., Lu, X. & Ruden, D. M. J.  
552 F. 2012 A program for annotating and predicting the effects of single nucleotide polymorphisms, SnpEff:  
553 SNPs in the genome of *Drosophila melanogaster* strain w1118; iso-2; iso-3. *Fly* 6, 80-92.  
554 (DOI:<https://doi.org/10.4161/fly.19695>).

555 [40] Choi, Y. & Chan, A. P. J. B. 2015 PROVEAN web server: a tool to predict the functional effect of amino  
556 acid substitutions and indels. *Bioinformatics* 31, 2745-2747.  
557 (DOI:<https://doi.org/10.1093/bioinformatics/btv195>).

558 [41] Dong, X., Li, J., He, J., Liu, W., Jiang, L., Ye, Y. & Wu, C. 2016 Anti-infective mannose receptor immune  
559 mechanism in large yellow croaker (*Larimichthys crocea*). *Fish & Shellfish Immunology* 54, 257-265.  
560 (DOI:<https://doi.org/10.1016/j.fsi.2016.04.006>).

561 [42] Wentzel, A. S., Petit, J., van Veen, W. G., Fink, I. R., Scheer, M. H., Piazzon, M. C., Forlenza, M., Spaink,  
562 H. P. & Wiegertjes, G. F. 2020 Transcriptome sequencing supports a conservation of macrophage  
563 polarization in fish. *Scientific Reports* 10, 13470. (DOI:<https://doi.org/10.1038/s41598-020-70248-y>).

564 [43] Layton, K. K. S., Snelgrove, P. V. R., Dempson, J. B., Kess, T., Lehnert, S. J., Bentzen, P., Duffy, S. J.,  
565 Messmer, A. M., Stanley, R. R. E., DiBacco, C., et al. 2021 Genomic evidence of past and future climate-  
566 linked loss in a migratory Arctic fish. *Nature Climate Change* 11, 158-165.  
567 (DOI:<https://doi.org/10.1038/s41558-020-00959-7>).

568 [44] Liu, P.-f., Du, Y., Meng, L., Li, X., Yang, D. & Liu, Y. 2019 Phosphoproteomic analyses of kidneys of  
569 Atlantic salmon infected with *Aeromonas salmonicida*. *Scientific Reports* 9, 2101.  
570 (DOI:<https://doi.org/10.1038/s41598-019-38890-3>).

571 [45] Shi, G., Abbott, K. N., Wu, W., Salter, R. D. & Keyel, P. A. 2017 Dnase1L3 Regulates Inflammasome-  
572 Dependent Cytokine Secretion. 8. (DOI:<https://doi.org/10.3389/fimmu.2017.00522>).

573 [46] Szymura, S. J., Bernal, G. M., Wu, L., Zhang, Z., Crawley, C. D., Voce, D. J., Campbell, P.-A., Ranoa, D. E.,  
574 Weichselbaum, R. R. & Yamini, B. 2020 DDX39B interacts with the pattern recognition receptor pathway to  
575 inhibit NF- $\kappa$ B and sensitize to alkylating chemotherapy. *BMC Biology* 18, 32.  
576 (DOI:<https://doi.org/10.1186/s12915-020-0764-z>).

577 [47] Schaal S., Haller B., Lotterhos K. 2022 Inversion Invasions: when the genetic basis of local adaptation is  
578 concentrated within inversions in the face of gene flow. *Philosophical Transactions of the Royal Society B X*,  
579 X. (DOI:<https://doi.org/10.1098/rstb.2021.0200>)

580 [48]. Stenløkk K, Saitou M, Rud-Johansen L, Nome T, Moser M, Árnýasi M, Kent M, Barson NJ, Lien S. 2022  
581 The emergence of supergenes from inversions in Atlantic salmon. *Figshare*. (doi:10.6084/m9.  
582 figshare.c.5983514)

583